

# Association of Upregulated Angiogenic Cytokines With Choroidal Abnormalities in Chronic Central Serous Chorioretinopathy

Nobuhiro Terao,<sup>1</sup> Hideki Koizumi,<sup>2</sup> Kentaro Kojima,<sup>1</sup> Tetsuya Yamagishi,<sup>1</sup> Kenji Nagata,<sup>1</sup> Koji Kitazawa,<sup>1</sup> Yuji Yamamoto,<sup>1</sup> Kengo Yoshii,<sup>3</sup> Asako Hiraga,<sup>4</sup> Munetoyo Toda,<sup>4</sup> Shigeru Kinoshita,<sup>4</sup> Chie Sotozono,<sup>1</sup> and Junji Hamuro<sup>1</sup>

<sup>1</sup>Department of Ophthalmology, Kyoto Prefectural University of Medicine, Kyoto, Japan

<sup>2</sup>Department of Ophthalmology, University of the Ryukyus, Okinawa, Japan

<sup>3</sup>Department of Mathematics and Statistics in Medical Sciences, Kyoto Prefectural University of Medicine, Kyoto, Japan

<sup>4</sup>Department of Frontier Medical Science and Technology for Ophthalmology, Kyoto Prefectural University of Medicine, Kyoto, Japan

Correspondence: Junji Hamuro, Department of Ophthalmology, Kyoto Prefectural University of Medicine, 465 Kajii-cho, Hirokoji-agaru, Kawaramachi-dori, Kamigyo-ku, Kyoto 602-0841, Japan; jshimo@koto.kpu-m.ac.jp.

Submitted: August 14, 2018

Accepted: November 12, 2018

Citation: Terao N, Koizumi H, Kojima K, et al. Association of upregulated angiogenic cytokines with choroidal abnormalities in chronic central serous chorioretinopathy. *Invest Ophthalmol Vis Sci.* 2018;59:5924–5931. <https://doi.org/10.1167/iovs.18-25517>

**PURPOSE.** To clarify the distinct molecular pathogenesis of central serous chorioretinopathy (CSC) and pachychoroid neovascularopathy (PNV).

**METHODS.** Aqueous humor (AH) was collected from 18 acute CSC, 20 chronic CSC, and 20 PNV patients. Concentrations of 30 cytokines in the AH were analyzed using a multiplex bead immunoassay, and the cytokine profiles were compared among these three groups of patients. The areas of choroidal vascular hyperpermeability (CVH) and choroidal thickness (CT), including measurement of the vascular layers, were investigated to analyze the features of choroidal abnormality in acute CSC, chronic CSC, and PNV. Additionally, associations between cytokine profiles and choroidal abnormalities were analyzed.

**RESULTS.** Proinflammatory cytokines, IL-6 and IL-8 were significantly upregulated in the chronic CSC group compared with the acute CSC or PNV groups. Angiogenic cytokines and VEGF-A were upregulated at levels that almost reached significance along with disease progression from acute to chronic CSC, whereas the upregulation was not significant from chronic CSC to PNV. In the chronic CSC group, strong positive correlations were confirmed between VEGF-A and placental growth factor (PIGF) ( $r = 0.75$ ,  $P < 0.001$ ) and IL-6 and VEGF-A ( $r = 0.74$ ,  $P < 0.001$ ), and angiogenesis-related cytokines were positively correlated with the typical choroidal abnormalities, areas of CVH, mean CT, and mean large choroidal vessel layer thickness. However, there was no association between these choroidal abnormality parameters and AH cytokines in the PNV group.

**CONCLUSIONS.** The results suggest that choroidal abnormalities in chronic CSC may be associated with upregulated angiogenesis.

**Keywords:** central serous chorioretinopathy, pachychoroid neovascularopathy, aqueous humor, cytokine, pachychoroid, choroidal abnormality, angiogenesis

The term “pachychoroid” describes a collection of choroidal abnormalities accompanied by increased choroidal thickness (CT), large dilation of choroidal vessels, and choroidal vascular hyperpermeability (CVH).<sup>1–3</sup> The pachychoroid is considered to be associated with the development of a spectrum of clinical diseases, including pachychoroid pigment epitheliopathy (PPE),<sup>1</sup> central serous chorioretinopathy (CSC), polypoidal choroidal vasculopathy,<sup>3</sup> and pachychoroid neovascularopathy (PNV).<sup>2</sup>

CSC is characterized by well-defined serous detachment of the neurosensory retina at the posterior pole.<sup>4</sup> CSC occurs predominantly in men between 30 and 60 years of age.<sup>5,6</sup> Although CSC cases are categorized into acute or chronic phases, there are no standardized criteria for defining the two sequences. Most previous studies have described chronic CSC as visual dysfunction lasting more than 6 months.<sup>7,8</sup>

Acute CSC causes symptoms such as visual disturbance, central scotoma, metamorphopsia, or micropsia. However, the visual prognosis is considered good, and serous retinal detachment (SRD) is often absorbed spontaneously within a few months.<sup>9,10</sup>

Chronic CSC is more common in the elderly, but acute CSC is not restricted to this age group. Chronic CSC is accompanied by recurrent SRD and extensive atrophy of the RPE. When atrophy occurs in the macular region, visual prognosis is poor. Recurrent or persistent retinal detachment leads to photoreceptor death and may result in permanent visual loss.

PNV is a newly proposed clinical entity that differs from AMD with type 1 choroidal neovascularization (CNV) secondary to CSC and PPE.<sup>2</sup> Recently, we published the new findings that the cytokine profiles in aqueous humor (AH) of PNV and neovascular AMD are distinct, and that angiogenic factors and



proinflammatory cytokines may play distinct roles in the pathogenesis of PNV and AMD.<sup>11</sup>

It is well recognized that type 1 CNV occurs in eyes with long-term CSC,<sup>12,13</sup> but it can also occur in the absence of subretinal fluid. Some studies have speculated that the pathological progression of pachychoroid is conversion from acute CSC to chronic CSC or from PPE and eventually to PNV<sup>14,15</sup>; however, not all patients with acute CSC develop chronic CSC, nor do all chronic CSC and PPE patients develop PNV. The molecular mechanism that accounts for these distinct disease progressions has not been fully explained.

Many clinical studies targeting the choroid have been conducted since Gass<sup>4</sup> suggested choroidal abnormality as the primary cause of CSC pathogenesis in 1967. Several studies have shown that choroidal filling delay, choroidal vascular dilation, and CVH can be observed in CSC.<sup>16–20</sup> Choroid in patients with CSC was thicker than that in healthy subjects,<sup>21,22</sup> and dilation of the large choroidal vessels accounted for the thickened choroid.<sup>23,24</sup> Based on these clinical findings, the major cause of CSC is presumed to be increased choroidal tissue hydrostatic pressure related to choroidal abnormalities such as CVH, choroidal thickening, and dilated choroidal vessels. Research on PNV, however, is currently in progress. Current studies on PNV have speculated that ischemia in the choriocapillaris or dysfunction of the RPE results in the formation of abnormal vascular networks.<sup>2,25,26</sup> Despite many studies on choroidal imaging, little is understood about the underlying molecular pathology in the choroidal abnormality, which may be a primary cause of CSC and PNV.

In this study, we analyzed cytokine profiles in the AH of acute CSC, chronic CSC, and PNV patients to address the distinct molecular pathogenesis of pachychoroid spectrum disease. In addition, associations between cytokine profiles and choroidal abnormalities were analyzed for the three groups.

## METHODS

This was a prospective, comparative control study conducted in a single institution; the study was approved by the institutional review board of the Kyoto Prefectural University of Medicine and was conducted in accordance with the tenets of the Declaration of Helsinki. Written informed consent was obtained from all participants following provision of a detailed explanation of the study protocol, including AH collection.

### Study Population

A total of 57 patients were recruited from the retina clinic in the Department of Ophthalmology, Kyoto Prefectural University of Medicine University Hospital, between January 2016 and February 2017. Of these, 18 patients had treatment-naïve acute CSC, 20 patients had treatment-naïve chronic CSC, and 19 patients had treatment-naïve PNV.

Patients with a history of systemic diabetes, collagen diseases, cardiovascular diseases, cerebrovascular diseases, or systemic corticosteroid medications were excluded from the study. Eyes with a history of any other retinal diseases; uveitis; glaucoma, including ocular hypertension with any antiglaucoma eye drops; intraocular surgery, including cataract surgery; or high myopia (spherical equivalent less than  $-6$  diopters or axial length  $>26.5$  mm) were also excluded from the study. In bilateral cases, left eyes were selected.

At the first examination, all patients underwent an extensive ophthalmic assessment with refraction, best-corrected visual acuity (BCVA) testing with Landolt C charts, measurement of the axial length, slit-lamp biomicroscopy with or without a contact lens, color fundus photography,

fluorescein angiography (FA), indocyanine green angiography (ICGA), fundus autofluorescence (FAF) photography, and spectral-domain or swept-source optical coherence tomography (SD- or SS-OCT). The presence or absence of CNV was determined via funduscopy, OCT, and angiographic findings. In cases in which CNV was uncertain, OCT angiography was also performed to conclusively identify CNV.

### Diagnosis of Acute CSC, Chronic CSC, and PNV

The CSC diagnosis was based on the presence of subretinal fluid involving the macula, together with confirmation of leaks from the RPE during FA. CVH appeared as hyperfluorescence in the late phase of ICGA.

Acute CSC (Fig. 1) was defined on the basis of the presence of clinical features as follows: (1) FA showing the typical pattern for one or several leakage points at the level of the RPE; (2) lack of evidence of wide hypo-autofluorescence (RPE damage) other than those leakage points on an FAF image; and (3) symptoms lasting less than 6 months. Chronic CSC (Fig. 1) was defined as the presence of persistent SRD for longer than 6 months and/or widespread areas of leakage from wide areas of RPE damage seen with FA.

PNV (Fig. 1) was diagnosed using the following criteria drawn from previous reports<sup>2,3,11,27,28</sup>: (1) type 1 CNV detected in either or both eyes; (2) no or only nonextensive drusen (total area  $\leq 125$   $\mu\text{m}$  circle) or hard drusen ( $\leq 63$   $\mu\text{m}$ ) in both eyes (Age-Related Eye Disease Study: Category 1, no AMD)<sup>29</sup>; (3) CVH detected in the late phase of ICGA; (4) dilated choroidal vessels below the type 1 CNV detected by ICGA and SD- or SS-OCT; and (5) presence of CSC- or PPE-related RPE abnormalities independent of CNV lesions detected by FAF or a history of CSC.

When the experienced physician was unable to establish a definitive diagnosis of chronic CSC or PNV, these confusing cases, including asymptomatic (nonleaky) vascular structure, were excluded from this study.

### Collection of AH

AH was obtained from CSC patients on the first visit, and for the PNV patients, it was obtained before an intravitreal injection of aflibercept. Before the paracentesis of the anterior chamber, the eyes were sterilized with povidone iodine and washed with saline. A specially designed 30-gauge needle integrated with a disposable pipette (Nipro, Osaka, Japan), as described in a previous study,<sup>30</sup> was used to withdraw AH. All of the procedures were undertaken carefully, avoiding any contamination, including blood. Approximately 150  $\mu\text{L}$  of the collected AH was immediately stored at  $-80^{\circ}\text{C}$  until cytokine analysis.

### Image Analysis

The presence of a complete posterior vitreous detachment (PVD) was determined using the SD- or SS-OCT images. We defined eyes as having a complete PVD if the detached vitreous was identified in vertical and horizontal scans or if there was a total absence of the posterior hyaloid. A descending tract was defined as a downward leading swath of decreased autofluorescence originating from the posterior pole and extending below the level of the inferior arcade. The presence of a descending tract was confirmed via FAF images. The presence of CVH was determined by two retinal specialists (N.T. and T.Y.). CVH appeared as multifocal hyperfluorescence in the middle and late phases of ICGA. The two specialists were blinded to the clinical findings, and CVH was determined only when both retinal specialists made the same judgment. The

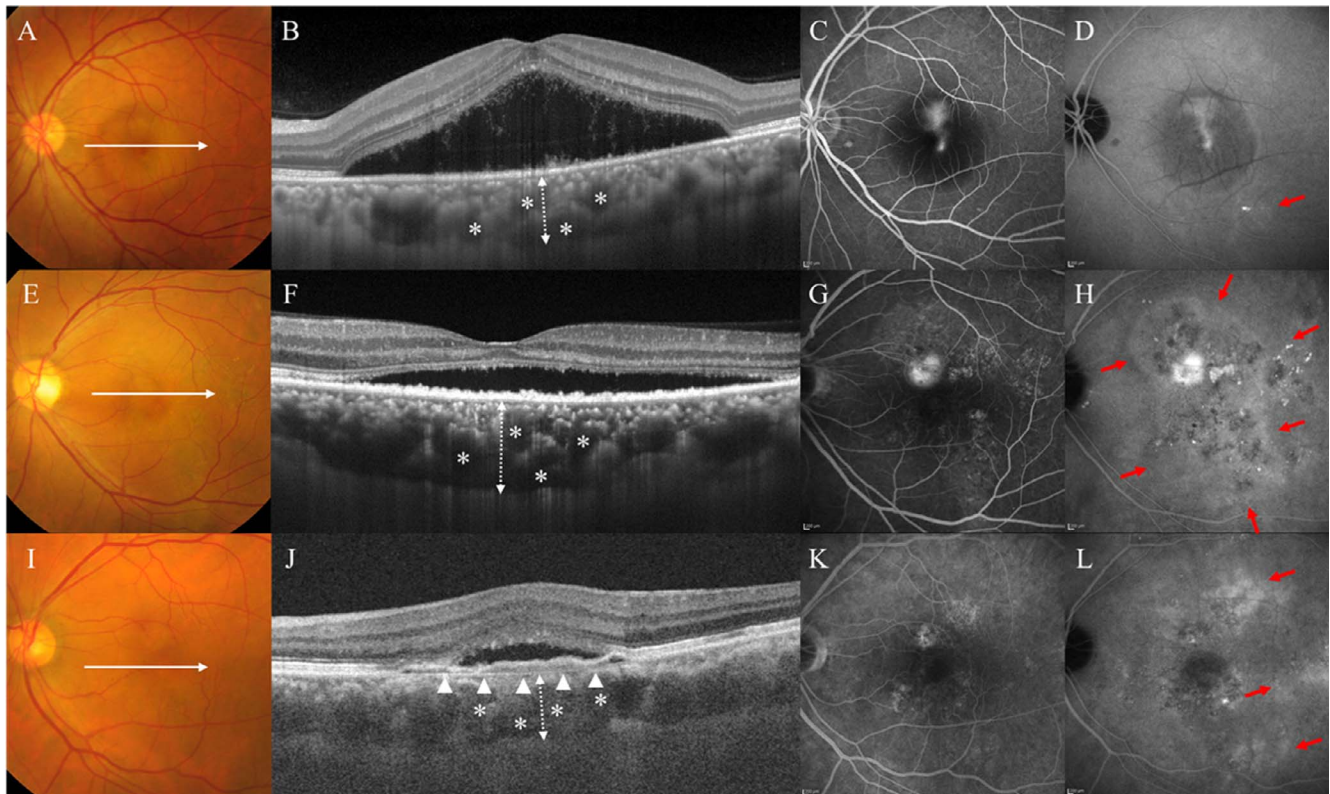


**FIGURE 1.** (A) Left eye of a 41-year-old male with acute CSC. Color fundus photography revealed SRD. (B) OCT along the *white lines* demonstrated SRD and thickened choroid (*dashed double-headed arrow*) with largely dilated choroidal vessels (*asterisks*). (C) FA revealed a focal leak in the central macula. (D) ICGA in the late phase revealed typical CVH (*red arrow*). (E) Left eye of a 68-year-old male with chronic CSC. Color fundus photography revealed SRD. (F) OCT along the *white lines* demonstrated SRD and thickened choroid (*dashed double-headed arrow*) with largely dilated choroidal vessels (*asterisks*). (G) FA revealed diffuse leakages in the macular area. (H) ICGA in the late phase revealed a multifocal area of CVH (*red arrows*). (I) Left eye of a 60-year-old male with PNV. Color fundus photography revealed SRD and absence of drusen. (J) OCT along the *white lines* demonstrated type-1 CNV (*arrowheads*) with SRD. There is thickening of the choroid (*dashed double-headed arrow*), with largely dilated choroidal vessels (*asterisks*) beneath the type-1 CNV. (K) FA revealed granular leakage of the dye in the macular area. (L) ICGA in the late phase revealed multifocal area of CVH (*red arrows*).

area of CVH was measured manually in each of the late-phase ICGA images within a range of  $30 \times 30$  degrees, using the draw region tool in the Heidelberg Retina Angiograph 2 (Fig. 2).

For choroidal layer analysis, we used a method described previously by Branchini et al.<sup>31</sup> We evaluated a horizontal OCT B-scan image and defined a layer of choroid with vessels with a diameter larger than  $100 \mu\text{m}$  as a large choroidal vessel layer (LCVL). The thickness of the LCVL was measured from the inner boundary of the LCVL to the inner wall of the sclera. The inner layer of the choroid was defined as the choriocapillaris + a medium choroidal vessel layer (CC + MCVL), the thickness of which was measured as the distance of Bruch's membrane to the inner boundary of the LCVL. In this study, CT, CC + MCVL, and LCVL were measured at three points: beneath the fovea,  $750 \mu\text{m}$  nasal from the fovea, and  $750 \mu\text{m}$  temporal from the fovea (Fig. 2). We averaged the data from the three points and defined the results as mean CT, mean CC + MCVL, and mean LCVL.

### Multiplex Analysis of Cytokines in AH

Concentrations of 30 different cytokines in the AH were analyzed using a Bio-Plex multiple assay (Bio-Plex Multiplex Immunoassay System; Bio-Rad Laboratories, Hercules, CA, USA). The measured cytokines were basic fibroblast growth factor (bFGF), eotaxin, granulocyte colony-stimulating factor (G-CSF), granulocyte macrophage colony-stimulating factor

(GM-CSF), IFN- $\gamma$ , IL-1 $\beta$ , IL-1ra, IL-2, IL-4, IL-5, IL-6, IL-7, IL-8, IL-9, IL-10, IL-12, IL-13, IL-15, IL-17, interferon- $\gamma$ -inducible protein (IP-10), monocyte chemoattractant protein (MCP)-1, macrophage inflammatory protein (MIP)-1 $\alpha$ , MIP-1 $\beta$ , platelet-derived growth factor (PDGF)-BB, regulated upon activation normal T-cell expressed and secreted (RANTES), TNF- $\alpha$ , VEGF-A, VEGF-C, VEGF-D, and placental growth factor (PlGF). The analysis was performed according to the manufacturer's instructions. Standard curves were generated using the Bio-Plex TM 200 System (Version 6.1; Bio-Rad Laboratories).

### Statistical Analysis

Statistical analysis was performed using JMP Pro V.11.2.0 software (SAS Institute, Cary, NC, USA) and the R statistical package (version 3.4.1 for Windows; Vienna, Austria). A *P* value less than 0.05 was accepted as statistically significant. Unless otherwise stated, the results are expressed as the median and interquartile range (IQR), and categorical data were assessed using Fisher's exact test. The statistical significance of the difference in the demographic and clinical characteristics data, as well as the cytokine concentrations in the three groups, was calculated using the Kruskal-Wallis test. Subsequently, cytokines with significant differences were analyzed using the Steel-Dwass method. Spearman's rank correlation coefficients were used to assess the relationships between cytokine concentrations for the three groups and

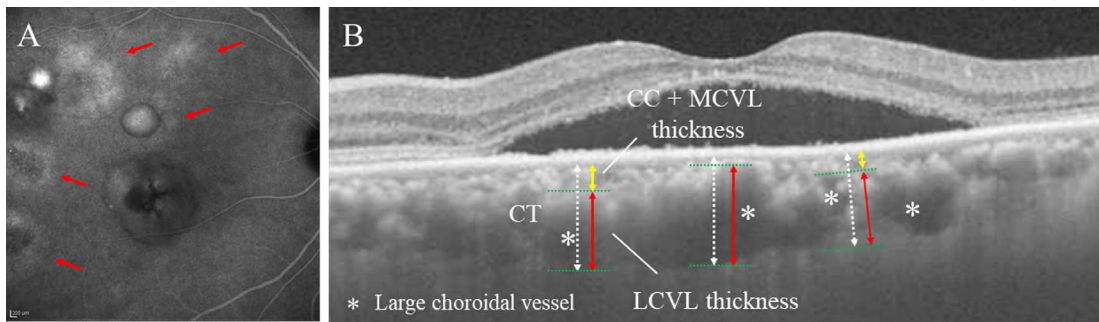


**FIGURE 2.** (A) A 46-year-old male with chronic CSC. Indocyanine green angiography in the late phase showed multifocal area of CVH (red arrows). Area of CVH was 11.67 mm<sup>2</sup>. (B) A 50-year-old male with chronic CSC. The mean CT (dashed white double-headed arrows), the mean LCVL (red double-headed arrows), and the mean CC + MCVL (yellow double-headed arrows) thicknesses were 327 μm, 278 μm, and 49 μm, respectively.

between each cytokine concentration and area of CVH, mean CT, and mean LCVL thickness for the three groups.

**RESULTS**

The demographic and clinical characteristics for the three groups are summarized in Table 1. There were significant differences in age ( $P < 0.01$ ), BCVA ( $P = 0.01$ ), CVH ( $P = 0.02$ ), and mean LCVL thickness ( $P = 0.02$ ) among the three groups, confirmed by the Kruskal-Wallis test. The sex, spherical equivalent, axial length, completion of PVD, rate of descending tract, and mean CT and mean CC + MCVL thickness were not different among the three groups.

Among the 30 cytokines analyzed, 10 cytokines (bFGF, GM-CSF, IL-1ra, IL-6, IL-8, IP-10, MCP-1, MIP-1β, VEGF-A, and PIGF) were detected in all three groups, whereas the other 20 cytokines were below detectable levels. In this study, eight cytokines (bFGF, GM-CSF, IL-6, IL-8, IP-10, MCP-1, VEGF-A, and PIGF) that were stably detected in all AH were used for statistical study (Table 2).

There were significant differences in concentrations of IL-6 ( $P < 0.01$ ), IL-8 ( $P = 0.01$ ), MCP-1 ( $P = 0.04$ ), bFGF ( $P = 0.05$ ), and GM-CSF ( $P = 0.02$ ) among the three groups, as determined by the Kruskal-Wallis test. Figure 2 shows the results of the Steel-Dwass analysis of these eight cytokines. IL-6 concentration in the chronic CSC group was significantly higher than that in the acute CSC group ( $P < 0.01$ ). IL-8 concentration in the chronic CSC group was significantly higher than that in the

PNV group ( $P = 0.02$ ). There was no significant difference in MCP-1 concentration among the three groups. The bFGF and GM-CSF concentrations in the acute CSC group were significantly higher than those in the PNV group ( $P = 0.05$ ,  $P = 0.02$ , respectively).

Similar differences in these cytokines among the three groups were observed via Spearman's rank correlation coefficient (Table 3). With the acute CSC group, there was a strong positive correlation between bFGF and GM-CSF concentrations ( $r = 0.70$ ,  $P = 0.001$ ), as well as a negative correlation between IP-10 and VEGF-A concentrations ( $r = -0.50$ ,  $P = 0.034$ ). In the chronic CSC group, there were strong positive correlations between VEGF-A and PIGF concentrations ( $r = 0.75$ ,  $P < 0.001$ ), IL-6 and VEGF-A concentrations ( $r = 0.74$ ,  $P < 0.001$ ), and bFGF and GM-CSF concentrations ( $r = 0.66$ ,  $P = 0.002$ ), whereas moderate positive correlations were observed between MCP-1 and IP-10 concentrations ( $r = 0.56$ ,  $P = 0.011$ ), IL-8 and MCP-1 concentrations ( $r = 0.53$ ,  $P = 0.018$ ), IL-6 and PIGF concentrations ( $r = 0.52$ ,  $P = 0.0181$ ), and bFGF and VEGF-A concentrations ( $r = 0.45$ ,  $P = 0.047$ ). In the PNV group, there were moderate positive correlations between VEGF-A and PIGF concentrations ( $r = 0.57$ ,  $P = 0.010$ ), bFGF and GM-CSF concentrations ( $r = 0.56$ ,  $P = 0.012$ ), IL-6 and MCP-1 concentrations ( $r = 0.49$ ,  $P = 0.034$ ), IL-8 and MCP-1 concentrations ( $r = 0.46$ ,  $P = 0.050$ ), and IP-10 and VEGF-A concentrations ( $r = 0.46$ ,  $P = 0.045$ ). There was a moderate negative correlation between GM-CSF and PIGF concentrations ( $r = -0.50$ ,  $P = 0.030$ ).

**TABLE 1.** Demographic and Clinical Characteristics Among the Three Groups

	CSC			P
	Acute	Chronic	PNV	
n	18	20	19	
Age, y	45.5 (41.0, 55.3)	54.0 (50.0, 61.8)	69.0 (59.0, 74.0)	<b>&lt;0.01*</b>
Female sex, n (%)	2 (11.1%)	3 (15.0%)	4 (22.2%)	0.82†
BCVA, logMAR	0.05 (-0.08, 0.17)	0.07 (0.00, 0.47)	0.30 (0.10, 0.40)	<b>0.01*</b>
Spherical equivalent, diopter	-0.750 (-1.875, 0.250)	-0.688 (-1.875, 0.250)	-0.250 (-1.875, 0.625)	0.75*
Axial length, mm	23.6 (22.94, 24.63)	23.58 (22.84, 24.38)	23.61 (22.90, 24.74)	0.95*
Complete PVD, n (%)	1 (5.6%)	5 (25.0%)	6 (31.6%)	0.13†
Descending tract, n (%)	0 (0%)	4 (20.0%)	2 (10.5%)	0.17†
CVH, mm <sup>2</sup>	5.60 (3.60, 13.33)	16.45 (7.52, 25.92)	13.7 (9.63, 26.14)	<b>0.02*</b>
Mean CT, μm	373 (285, 472)	414 (338, 486)	326 (276, 395)	0.06*
Mean CC+MCVL thickness, μm	92 (52, 125)	62 (51, 97)	67 (54, 99)	0.44*
Mean LCVL thickness, μm	308 (206, 348)	353 (280, 400)	276 (209, 318)	<b>0.02*</b>

Values are the median (interquartile range).  $< 0.05$  was considered significant (bold).

\* Kruskal-Wallis test.

† Fisher's exact test.

TABLE 2. Levels of Eight Cytokines in the AH Among the Three Groups

	CSC			P*
	Acute	Chronic	PNV	
n	18	20	19	
IL-6, pg/mL	3.16 (2.36, 4.73)	8.09 (3.59, 19.83)	2.91 (2.08, 9.16)	<0.01
IL-8, pg/mL	5.54 (4.66, 7.85)	7.85 (6.65, 11.71)	5.48 (3.06, 6.49)	0.01
MCP-1, pg/mL	203.77 (170.00, 241.55)	238.17 (195.83, 278.16)	118.69 (135.62, 242.03)	0.04
IP-10, pg/mL	125.23 (85.77, 212.57)	141.24 (109.49, 259.05)	123.22 (61.14, 228.32)	0.60
bFGF, pg/mL	18.62 (14.64, 20.86)	14.12 (8.95, 20.24)	10.70 (7.62, 17.62)	0.05
GM-CSF, pg/mL	79.75 (45.49, 87.89)	58.86 (43.60, 74.20)	43.92 (27.31, 59.94)	0.02
VEGF-A, pg/mL	114.95 (94.89, 146.01)	146.51 (113.42, 202.04)	156.75 (105.88, 179.44)	0.06
PIGF, pg/mL	3.13 (1.30, 4.34)	3.61 (1.98, 4.57)	4.51 (2.70, 5.61)	0.23

Values are the median (interquartile range). < 0.05 was considered significant (bold).  
\* Kruskal-Wallis test.

Table 4 shows that the area of CVH, the mean CT, and the mean LCVL thickness correlated with multiple proangiogenic cytokines in the acute and chronic CSC groups. In the acute CSC group, there were positive correlations between CVH and MCP-1 concentrations ( $r = 0.80, P < 0.001$ ), between mean CT and bFGF ( $r = 0.48, P = 0.043$ ) and GM-CSF concentrations ( $r = 0.51, P = 0.030$ ), and between mean LCVL thickness and GM-CSF concentration ( $r = 0.52, P = 0.028$ ). In the chronic CSC group, there were positive correlations between CVH and IL-6 ( $r = 0.56, P = 0.011$ ) and VEGF-A concentrations ( $r = 0.45, P = 0.048$ ); between mean CT and IL-6 ( $r = 0.53, P = 0.015$ ), bFGF ( $r = 0.52, P = 0.019$ ), GM-CSF ( $r = 0.45, P = 0.046$ ), and VEGF-A concentrations ( $r = 0.47, P = 0.038$ ); and between mean LCVL thickness and IL-6 ( $r = 0.49, P = 0.028$ ) and bFGF concentrations ( $r = 0.46, P = 0.042$ ). In the PNV group, there

were no cytokines correlated with CVH, mean CT, or mean LCVL thickness.

DISCUSSION

This study provides the first comprehensive analysis of pachychoroid spectrum diseases including CSC and PNV. Proinflammatory cytokines were significantly upregulated in the chronic CSC group compared with the acute CSC and the PNV groups, whereas VEGF-A was upregulated but did not quite reach significance along with disease progression from acute CSC to chronic CSC. Upregulation from chronic CSC to PNV was not significant (Fig. 3).

Our results show that choroidal pathologies are associated with the AH cytokine profiles. Several studies have described

TABLE 3. Spearman's Rank Correlation Coefficient for Eight Cytokines Among the Three Groups

	IL-6	IL-8	MCP-1	IP-10	bFGF	GM-CSF	VEGF-A
Acute CSC							
IL-8	0.31	1.00					
MCP-1	0.11	0.45	1.00				
IP-10	0.18	0.09	0.23	1.00			
bFGF	-0.40	-0.02	0.10	-0.28	1.00		
GM-CSF	-0.26	-0.12	0.11	0.10	0.70†	1.00	
VEGF-A	0.19	0.13	-0.13	-0.50‡	0.23	-0.28	1.00
PIGF	-0.25	0.43	0.15	-0.29	0.32	0.02	0.24
Chronic CSC							
IL-8	0.24	1.00					
MCP-1	0.34	0.53‡	1.00				
IP-10	0.44	0.39	0.56‡	1.00			
bFGF	0.32	<0.01	0.17	-0.03	1.00		
GM-CSF	0.01	0.06	0.22	0.21	0.66†	1.00	
VEGF-A	0.74*	0.19	0.20	0.26	0.45‡	0.16	1.00
PIGF	0.52‡	0.24	0.10	0.18	0.34	-0.14	0.75*
PNV							
IL-8	0.41	1.00					
MCP-1	0.49‡	0.46‡	1.00				
IP-10	0.28	0.31	0.45	1.00			
bFGF	0.26	0.42	-0.03	-0.12	1.00		
GM-CSF	0.01	0.08	-0.04	-0.37	0.56‡	1.00	
VEGF-A	0.27	0.29	0.06	0.46‡	0.25	-0.25	1.00
PIGF	0.33	0.40	-0.01	0.38	0.25	-0.50‡	0.57‡

P < 0.05 was considered significant (bold).

\* P < 0.001.

† P < 0.01.

‡ P < 0.05.

TABLE 4. Spearman's Rank Correlation Coefficient Between CVH and Choroidal Layer and Eight Cytokine Levels Among the Three Groups

	Vs. CVH			Vs. Mean CT			Vs. Mean LCVL Thickness		
	CSC		PNV	CSC		PNV	CSC		PNV
	Acute	Chronic		Acute	Chronic		Acute	Chronic	
IL-6, pg/mL	0.12	<b>0.56†</b>	0.12	-0.08	<b>0.53†</b>	-0.07	<0.01	<b>0.49†</b>	-0.22
IL-8, pg/mL	0.42	0.20	0.20	0.03	0.30	-0.14	0.01	0.37	-0.19
MCP-1, pg/mL	<b>0.80*</b>	0.21	-0.09	0.06	0.19	-0.29	0.08	0.25	-0.24
IP-10, pg/mL	0.19	0.16	-0.15	-0.34	0.23	-0.06	-0.17	0.15	-0.01
bFGF, pg/mL	0.17	-0.23	0.39	<b>0.48†</b>	<b>0.52†</b>	-0.36	0.46	<b>0.46†</b>	-0.44
GM-CSF, pg/mL	0.25	-0.29	0.07	<b>0.51†</b>	<b>0.45†</b>	-0.28	<b>0.52†</b>	0.36	-0.40
VEGF-A, pg/mL	-0.11	<b>0.45†</b>	0.11	0.02	<b>0.47†</b>	0.15	-0.08	0.41	0.16
PIGF, pg/mL	0.06	0.14	0.16	0.11	0.30	0.29	0.03	0.27	0.26

P < 0.05 was considered significant (bold).

\* P < 0.001.

† P < 0.05.

correlations between cytokine levels in the AH and vitreous fluids.<sup>32,35</sup> The channel connecting Cloquet's canal and the posterior precortical vitreous pocket suggests that there is communication between the AH and the posterior precortical vitreous pocket.<sup>34,35</sup>

To date, no studies have shown the participation of inflammation in CSC pathology. Inflammatory markers and inflammatory cytokines have not been observed in biological samples (i.e., AH<sup>36-38</sup> and blood<sup>36,39</sup>) or pathological tissues.<sup>40</sup> In this study, the concentration of proinflammatory cytokines, such as IL-6, IL-8, MCP-1, and IP-10, in the chronic CSC group tended to be higher than those in the acute CSC and PNV groups (Figs. 3A-D). In addition, Spearman's rank correlation coefficient clearly indicated that the correlations among these proinflammatory cytokines in the acute CSC group were significantly lower than those in the chronic CSC and PNV groups. These results may suggest that tissue inflammation, accompanied by infiltrates of inflammatory immune cells, such as macrophages, into the choroid-retinal tissues, may cause the

progression of CSC from acute to chronic. The prolonged presence of ectopic subretinal fluids may dysregulate the immune regulatory function of the RPE to induce aberrant macrophage activation, resulting in the upregulated production of proinflammatory cytokines, such as IL-6, IL-8, and MCP-1. This kind of cell-to-cell interaction between the RPE and macrophages (increased production of IL-6, IL-8, MCP-1, and VEGF) was reported recently by one of the co-authors.<sup>41</sup>

However, cytokines maintaining constitutive hematopoiesis, such as bFGF and GM-CSF,<sup>42</sup> tended to decrease along with progression of the disease from acute to chronic CSC and, eventually, to PNV (Figs. 2E, 2F, Table 4). The bFGF was also a potent angiogenic factor with a pivotal role in the regeneration of various tissues,<sup>43</sup> whereas GM-CSF promotes hematopoiesis and the proliferation and differentiation of leukocytes. The microenvironmental changes in the anterior chamber resulting from pathological CNV formation in PNV may account for the dysregulated production of these cytokines relevant to the physiological homeostasis.

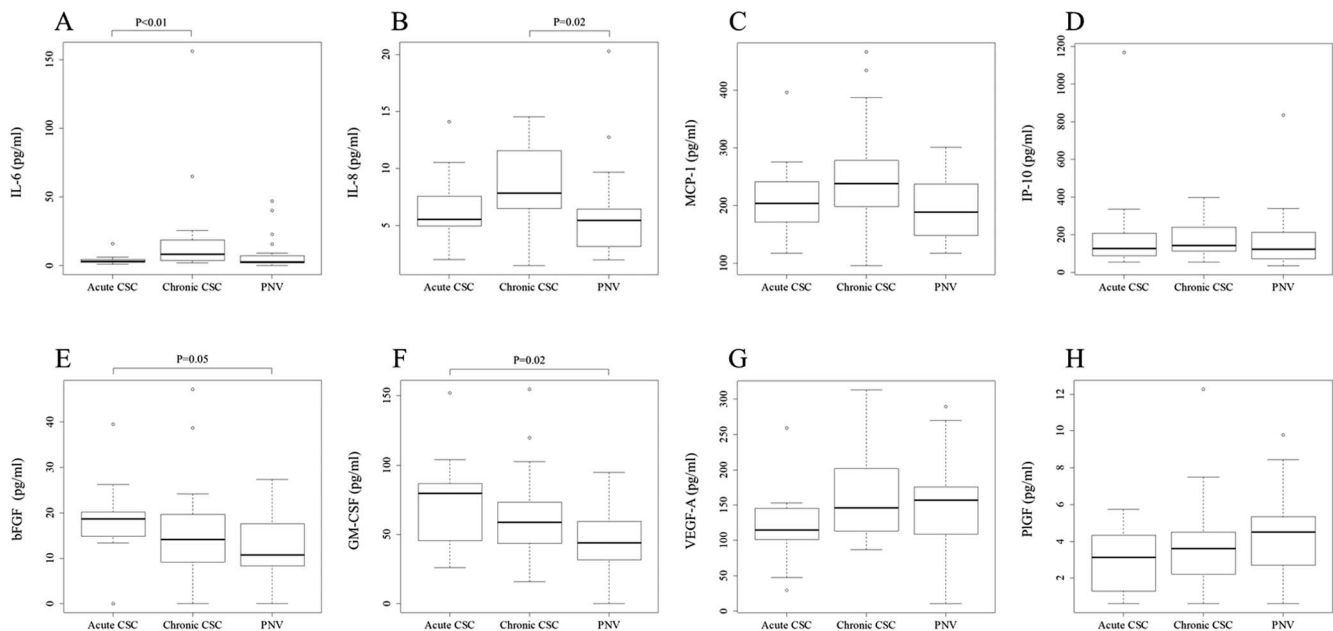


FIGURE 3. (A-H) Box-and-whisker plot of eight cytokines detected in the AH of patients in the acute CSC, chronic CSC, and PNV groups. Cytokine level is indicated on the left side of each plot. The middle lines represent the median value, the top part of the box represents the 75th percentile, and the bottom of the box represents the 25th percentile. The whiskers extend to 1.5 times the IQR. Open circles represent extreme values. The P values were obtained by using the Steel-Dwass Test. Only P < 0.05 is described.

VEGF may enhance choroidal hyperpermeability in CSC; however, in previous reports, VEGF levels in the AH of patients with CSC were not significantly increased compared with levels in control patients.<sup>36-38</sup> In this study, angiogenic cytokines, such as VEGF-A and PlGF, tended to increase gradually along with disease progression from acute to chronic CSC and, eventually, to PNV (Figs. 2G, 2H). In addition, Spearman's rank correlation coefficient clearly indicated the presence of significant correlations among the angiogenic cytokines in the chronic CSC group, whereas the correlations among these cytokines in the acute CSC groups were significantly lower. Anti-VEGF therapy has been reported as an effective treatment for chronic CSC<sup>44,45</sup> and PNV.<sup>27,46</sup> The gradual increase of VEGF and PlGF along with disease progression may suggest that CNV arises as a consequence of angiogenic cytokine accumulation, triggered by aberrant interaction between dysregulated RPE and macrophages.

The discrepancy between the average ages of the subjects in the three groups may have contributed to the observed tendency toward increased cytokines (Supplementary Table S1). However, the changes in cytokines may certainly be associated with the changes accompanying pachychoroid spectrum disease progression, because the chronic CSC group ( $r = 0.75$ ,  $P < 0.001$ ) showed a statistically significant stronger correlation with VEGF-A and PlGF than did the PNV group ( $r = 0.57$ ,  $P < 0.05$ ) with higher age.

In the chronic CSC groups, angiogenic cytokines positively correlated with the area of CVH, the mean CT, and the mean LCVL thickness (Table 4). The area of CVH showed a strong association with MCP-1 concentration in acute CSC. In chronic CSC, IL-6 and VEGF-A concentrations correlated with the area of CVH. The mean CT correlated with bFGF and GM-CSF concentrations in acute CSC, whereas IL-6 and VEGF concentrations, in addition to bFGF and GM-CSF concentrations, showed association with CT in chronic CSC. There was a similar trend, with a slightly lower correlation, between the mean LCVL thickness and cytokines. In contrast, there was no association between the choroidal abnormality parameters and cytokine concentrations in the PNV group. The strong association of the area of the CVH with MCP-1 concentration in acute CSC may indicate that recruitment of macrophages in the choroid may play a critical role in the induction of this clinical feature. The increase in choroidal abnormalities represented by CVH, mean CT, and mean LCVL thickness, together with the involvement of angiogenic cytokines, indicates that chronic CSC is a more advanced stage of the disease characterized by the aberrant angiogenesis process. PNV did not show any association with cytokines and may be the end stage of this clinical spectrum.

The concentration of cytokines in the anterior chamber is better analyzed on the basis of statistically classified and stratified parameters, such as the status of the vitreous cavity (presence or absence of PVD,<sup>47</sup> volume of the eyeball, and so on). In this study, axial length and the presence or absence of PVD were not different among the three groups. Further, there was no correlation between cytokine concentration and axial length nor any correlations showing a significant difference in the presence or absence of completion of PVD (Supplementary Tables S1, S2).

This study has several limitations. First, the diagnostic criteria for PNV may not be sufficient because of the lack of standard diagnostic criteria for this disease. Second, strictly controlled age matching is necessary to reach a generalizable conclusion. Third, cytokine profiles were measured only in AH. Considering the existing reports describing an association between CSC and hypercortisolemic<sup>48</sup> and serum plasminogen activator inhibitor 1 upregulation,<sup>39</sup> cytokine profiles should be better analyzed and compared in both AH and blood

simultaneously. Finally, research examining cytokine profiles in PPE with an increased number of cases is necessary to make the findings in this study more robust.

In conclusion, this study comprehensively analyzed cytokines in acute CSC, chronic CSC, and PNV, which are all along the pachychoroid disease spectrum. We have shown that choroidal abnormalities found in chronic CSC may be involved in the process of upregulated angiogenesis due to the dysregulated interaction between RPE and infiltrated macrophages. To better understand the molecular features of choroid abnormalities, it is necessary to further investigate the factors enhancing vascular permeability or vasoactivity, such as angiopoietin, in the process leading to PNV.

### Acknowledgments

Disclosure: **N. Terao**, None; **H. Koizumi**, None; **K. Kojima**, None; **T. Yamagishi**, None; **K. Nagata**, None; **K. Kitazawa**, None; **Y. Yamamoto**, None; **K. Yoshii**, None; **A. Hiraga**, None; **M. Munetoyo**, None; **S. Kinoshita**, None; **C. Sotozono**, None; **J. Hamuro**, None

### References

1. Warrow DJ, Hoang QV, Freund KB. Pachychoroid pigment epitheliopathy. *Retina*. 2013;33:1659-1672.
2. Pang CE, Freund KB. Pachychoroid neovascularopathy. *Retina*. 2015;35:1-9.
3. Balaratnasingam C, Lee WK, Koizumi H, Dansingani K, Inoue M, Freund KB. Polypoidal choroidal vasculopathy: a distinct disease or manifestation of another? *Retina*. 2016;36:1-8.
4. Gass JD. Pathogenesis of disciform detachment of the neuroepithelium. *Am J Ophthalmol*. 1967;63(Suppl):1-139.
5. Kitzmann AS, Pulido JS, Diehl NN, Hodge DO, Burke JP. The incidence of central serous chorioretinopathy in Olmsted County, Minnesota, 1980-2002. *Ophthalmology*. 2008;115:169-173.
6. Tsai DC, Chen SJ, Huang CC, et al. Risk of central serous chorioretinopathy in adults prescribed oral corticosteroids: a population-based study in Taiwan. *Retina*. 2014;34:1867-1874.
7. Yannuzzi LA. Central serous chorioretinopathy: a personal perspective. *Am J Ophthalmol*. 2010;149:361-363.
8. Zhao M, Zhang F, Chen Y, et al. A 50% vs 30% dose of verteporfin (photodynamic therapy) for acute central serous chorioretinopathy: one-year results of a randomized clinical trial. *JAMA Ophthalmol*. 2015;133:333-340.
9. Klein ML, Van Buskirk EM, Friedman E, Gragoudas E, Chandra S. Experience with nontreatment of central serous choroidopathy. *Arch Ophthalmol*. 1974;91:247-250.
10. Yannuzzi LA. Type-A behavior and central serous chorioretinopathy. *Retina*. 1987;7:111-131.
11. Terao N, Koizumi H, Kojima K, et al. Distinct aqueous humour cytokine profiles of patients with pachychoroid neovascularopathy and neovascular age-related macular degeneration. *Sci Rep*. 2018;8:10520.
12. Peiretti E, Ferrara DC, Caminiti G, Mura M, Hughes J. Choroidal neovascularization in Caucasian patients with longstanding central serous chorioretinopathy. *Retina*. 2015;35:1360-1367.
13. Hage R, Mrejen S, Krivosic V, Quentel G, Tadayoni R, Gaudric A. Flat irregular retinal pigment epithelium detachments in choroidal central serous chorioretinopathy and choroidal neovascularization. *Am J Ophthalmol*. 2015;159:890-903.e3.
14. Spaide RF, Campeas L, Haas A, et al. Central serous chorioretinopathy in younger and older adults. *Ophthalmology*. 1996;103:2070-2079; discussion 2079-2080.

15. Bonini Filho MA, de Carlo TE, Ferrara D, et al. Association of choroidal neovascularization and central serous chorioretinopathy with optical coherence tomography angiography. *JAMA Ophthalmol*. 2015;133:899-906.
16. Scheider A, Nasemann JE, Lund OE. Fluorescein and indocyanine green angiographies of central serous chorioretinopathy by scanning laser ophthalmoscopy. *Am J Ophthalmol*. 1993;115:50-56.
17. Piccolino FC, Borgia L. Central serous chorioretinopathy and indocyanine green angiography. *Retina*. 1994;14:231-242.
18. Prunte C. Indocyanine green angiographic findings in central serous chorioretinopathy. *Int Ophthalmol*. 1995;19:77-82.
19. Spaide RF, Hall L, Haas A, et al. Indocyanine green videoangiography of older patients with central serous chorioretinopathy. *Retina*. 1996;16:203-213.
20. Iida T, Kishi S, Hagimura N, Shimizu K. Persistent and bilateral choroidal vascular abnormalities in central serous chorioretinopathy. *Retina*. 1999;19:508-512.
21. Imamura Y, Fujiwara T, Margolis R, Spaide RF. Enhanced depth imaging optical coherence tomography of the choroid in central serous chorioretinopathy. *Retina*. 2009;29:1469-1473.
22. Maruko I, Iida T, Sugano Y, Ojima A, Sekiryu T. Subfoveal choroidal thickness in fellow eyes of patients with central serous chorioretinopathy. *Retina*. 2011;31:1603-1608.
23. Chung YR, Kim JW, Kim SW, Lee K. Choroidal thickness in patients with central serous chorioretinopathy: assessment of Haller and Sattler layers. *Retina*. 2016;36:1652-1657.
24. Sonoda S, Sakamoto T, Kuroiwa N, et al. Structural changes of inner and outer choroid in central serous chorioretinopathy determined by optical coherence tomography. *PLoS One*. 2016;11:e0157190.
25. Gallego-Pinazo R, Dolz-Marco R, Gomez-Ulla F, Mrejen S, Freund KB. Pachychoroid diseases of the macula. *Med Hypothesis Discov Innov Ophthalmol*. 2014;3:111-115.
26. Dansingani KK, Balaratnasingam C, Klufas MA, Sarraf D, Freund KB. Optical coherence tomography angiography of shallow irregular pigment epithelial detachments in pachychoroid spectrum disease. *Am J Ophthalmol*. 2015;160:1243-1254.e2.
27. Miyake M, Ooto S, Yamashiro K, et al. Pachychoroid neovascularopathy and age-related macular degeneration. *Sci Rep*. 2015;5:16204.
28. Takahashi A, Ooto S, Yamashiro K, et al. Pachychoroid Geographic Atrophy. *Ophthalmol Retina*. 2018;2:295-305.
29. Age-Related Eye Disease Study Research Group. The Age-Related Eye Disease Study system for classifying age-related macular degeneration from stereoscopic color fundus photographs: the Age-Related Eye Disease Study Report Number 6. *Am J Ophthalmol*. 2001;132:668-681.
30. Kitazawa K, Sotozono C, Koizumi N, et al. Safety of anterior chamber paracentesis using a 30-gauge needle integrated with a specially designed disposable pipette. *Br J Ophthalmol*. 2017;101:548-550.
31. Branchini LA, Adhi M, Regatieri CV, et al. Analysis of choroidal morphologic features and vasculature in healthy eyes using spectral-domain optical coherence tomography. *Ophthalmology*. 2013;120:1901-1908.
32. Aiello LP, Avery RL, Arrigg PG, et al. Vascular endothelial growth factor in ocular fluid of patients with diabetic retinopathy and other retinal disorders. *N Engl J Med*. 1994;331:1480-1487.
33. Noma H, Funatsu H, Yamasaki M, et al. Aqueous humor levels of cytokines are correlated to vitreous levels and severity of macular oedema in branch retinal vein occlusion. *Eye (Lond)*. 2008;22:42-48.
34. Itakura H, Kishi S, Li D, Akiyama H. Observation of posterior precortical vitreous pocket using swept-source optical coherence tomography. *Invest Ophthalmol Vis Sci*. 2013;54:3102-3107.
35. Itakura H, Kishi S, Li D, Akiyama H. En face imaging of posterior precortical vitreous pockets using swept-source optical coherence tomography. *Invest Ophthalmol Vis Sci*. 2015;56:2898-2900.
36. Lim JW, Kim MU, Shin MC. Aqueous humor and plasma levels of vascular endothelial growth factor and interleukin-8 in patients with central serous chorioretinopathy. *Retina*. 2010;30:1465-1471.
37. Shin MC, Lim JW. Concentration of cytokines in the aqueous humor of patients with central serous chorioretinopathy. *Retina*. 2011;31:1937-1943.
38. Jung SH, Kim KA, Sohn SW, Yang SJ. Cytokine levels of the aqueous humor in central serous chorioretinopathy. *Clin Exp Optom*. 2014;97:264-269.
39. Iijima H, Iida T, Murayama K, Imai M, Gohdo T. Plasminogen activator inhibitor 1 in central serous chorioretinopathy. *Am J Ophthalmol*. 1999;127:477-478.
40. Klien BA. Macular and extramacular serous chorioretinopathy. With remarks upon the role of an extrabulbar mechanism in its pathogenesis. *Am J Ophthalmol*. 1961;51:231-242.
41. Yamawaki T, Ito E, Mukai A, et al. The ingenious interactions between macrophages and functionally plastic retinal pigment epithelium cells. *Invest Ophthalmol Vis Sci*. 2016;57:5945-5953.
42. Metcalf D, Begley CG, Williamson DJ, et al. Hemopoietic responses in mice injected with purified recombinant murine GM-CSF. *Exp Hematol*. 1987;15:1-9.
43. Ornitz DM, Itoh N. The fibroblast growth factor signaling pathway. *Wiley Interdiscip Rev Dev Biol*. 2015;4:215-266.
44. Chung YR, Kim JW, Song JH, Park A, Kim MH. Twelve-month efficacy of intravitreal bevacizumab injection for chronic, atypical, or recurrent central serous chorioretinopathy [published online ahead of print October 26, 2017]. *Retina*. doi:10.1097/IAE.0000000000001917.
45. Pitcher JD III, Witkin AJ, DeCroos FC, Ho AC. A prospective pilot study of intravitreal aflibercept for the treatment of chronic central serous chorioretinopathy: the CONTAIN study. *Br J Ophthalmol*. 2015;99:848-852.
46. Matsumoto H, Hiroe T, Morimoto M, Mimura K, Ito A, Akiyama H. Efficacy of treat-and-extend regimen with aflibercept for pachychoroid neovascularopathy and Type 1 neovascular age-related macular degeneration. *Jpn J Ophthalmol*. 2018;62:144-150.
47. Nomura Y, Takahashi H, Tan X, Fujino Y, Kawashima H, Yanagi Y. Effect of posterior vitreous detachment on aqueous humor level of vascular endothelial growth factor in exudative age-related macular degeneration patients. *Graefes Arch Clin Exp Ophthalmol*. 2016;254:53-57.
48. Bouzas EA, Scott MH, Mastorakos G, Chrousos GP, Kaiser-Kupfer MI. Central serous chorioretinopathy in endogenous hypercortisolism. *Arch Ophthalmol*. 1993;111:1229-1233.